

A Spectral Time-Domain Method for Computational Electrodynamics

James V. Lambers^{1,*}

¹ *Department of Mathematics, University of Southern Mississippi, Hattiesburg, MS 39406-0001 USA*

Received 28 February 2009; Accepted (in revised version) 25 August 2009

Available online 18 November 2009

Abstract. Ever since its introduction by Kane Yee over forty years ago, the finite-difference time-domain (FDTD) method has been a widely-used technique for solving the time-dependent Maxwell's equations that has also inspired many other methods. This paper presents an alternative approach to these equations in the case of spatially-varying electric permittivity and/or magnetic permeability, based on Krylov subspace spectral (KSS) methods. These methods have previously been applied to the variable-coefficient heat equation and wave equation, and have demonstrated high-order accuracy, as well as stability characteristic of implicit time-stepping schemes, even though KSS methods are explicit. KSS methods for scalar equations compute each Fourier coefficient of the solution using techniques developed by Golub and Meurant for approximating elements of functions of matrices by Gaussian quadrature in the spectral, rather than physical, domain. We show how they can be generalized to coupled systems of equations, such as Maxwell's equations, by choosing appropriate basis functions that, while induced by this coupling, still allow efficient and robust computation of the Fourier coefficients of each spatial component of the electric and magnetic fields. We also discuss the application of block KSS methods to problems involving non-self-adjoint spatial differential operators, which requires a generalization of the block Lanczos algorithm of Golub and Underwood to unsymmetric matrices.

AMS subject classifications: 65M10, 78A48

Key words: Spectral methods, Gaussian quadrature, block Lanczos method, Maxwell's equations.

1 Introduction

We consider Maxwell's equation on the rectangle $[0, 2\pi]^3$, with periodic boundary con-

*Corresponding author.

URL: <http://www.math.usm.edu/lambers>

Email: James.Lambers@usm.edu (James V. Lambers)

ditions. Assuming nonconductive material with no losses, we have

$$\operatorname{div} \hat{\mathbf{E}} = 0, \quad \operatorname{div} \hat{\mathbf{H}} = 0, \quad (1.1)$$

$$\operatorname{curl} \hat{\mathbf{E}} = -\mu \frac{\partial \hat{\mathbf{H}}}{\partial t}, \quad \operatorname{curl} \hat{\mathbf{H}} = \varepsilon \frac{\partial \hat{\mathbf{E}}}{\partial t}, \quad (1.2)$$

where $\hat{\mathbf{E}}$, $\hat{\mathbf{H}}$ are the vectors of the electric and magnetic fields, and ε , μ are the electric permittivity and magnetic permeability, respectively. We assume that these two functions are smoothly varying in space.

By taking the curl of both sides of (1.2), we decouple the vector fields $\hat{\mathbf{E}}$ and $\hat{\mathbf{H}}$ and obtain the equations

$$\mu \varepsilon \frac{\partial^2 \hat{\mathbf{E}}}{\partial t^2} = \Delta \hat{\mathbf{E}} + \mu^{-1} \operatorname{curl} \hat{\mathbf{E}} \times \nabla \mu, \quad (1.3)$$

$$\mu \varepsilon \frac{\partial^2 \hat{\mathbf{H}}}{\partial t^2} = \Delta \hat{\mathbf{H}} + \varepsilon^{-1} \operatorname{curl} \hat{\mathbf{H}} \times \nabla \varepsilon. \quad (1.4)$$

In paper [26], Yee proposed the original finite-difference time-domain method for solving Eqs. (1.1) and (1.2). This method uses a staggered grid to avoid solving simultaneous equations for $\hat{\mathbf{E}}$ and $\hat{\mathbf{H}}$, and also removes numerical dissipation. However, because it is an explicit finite-difference scheme, its time step is constrained by the CFL condition. Nonetheless, it remains a widely used method to this day, and has inspired a host of related methods, including, for example, several that are based on spatial discretizations other than finite differences, such as a pseudospectral time-domain (PSTD) method [20], an FDTD-FEM hybrid method [22], and a one-step algorithm based on Chebyshev polynomial approximations [5]. In this paper, we introduce a new time-domain method for these equations.

In [18], a class of methods, called Krylov subspace spectral (KSS) methods, was introduced for the purpose of solving parabolic variable-coefficient PDE. These methods are based on techniques developed by Golub and Meurant in [7] for approximating elements of a function of a matrix by Gaussian quadrature in the *spectral* domain. In [11, 14], these methods were generalized to the second-order wave equation, for which these methods have exhibited even higher-order accuracy.

It has been shown in these references that KSS methods, by employing different approximations of the solution operator for each Fourier coefficient of the solution, achieve higher-order accuracy in time than other Krylov subspace methods (see, e.g., [13]) for stiff systems of ODE, and, as shown in [14], they are also quite stable, considering that they are explicit methods. In [15, 16], the accuracy and robustness of KSS methods were enhanced using block Gaussian quadrature.

It is our hope that the high-order accuracy achieved for the scalar wave equation can be extended to systems of coupled wave equations such as those described by Maxwell's equations. Section 2 reviews the main properties of KSS methods, including block KSS methods, as applied to the parabolic problems for which they were originally designed. Section 3 reviews their application to the wave equation, including previous convergence analysis. In Section 4, we discuss the modifications that

must be made to block KSS methods in order to apply them to Maxwell's equations, as well as issues that must be addressed in future work in order to obtain effective algorithms for solving more realistic problems involving these equations. Numerical results are presented in Section 5, and conclusions are stated in Section 6.

2 Krylov subspace spectral methods

We first review KSS methods, which are easier to describe for parabolic problems. Let $S(t)=\exp(-Lt)$ represent the exact solution operator of the problem

$$u_t + Lu = 0, \quad t > 0, \quad (2.1)$$

$$u(x, 0) = f(x), \quad 0 < x < 2\pi, \quad (2.2)$$

$$u(0, t) = u(2\pi, t), \quad t > 0. \quad (2.3)$$

The operator L is a second-order differential operator of the form

$$Lu = -(p(x)u_x)_x + q(x)u, \quad (2.4)$$

where $p(x)$ is a positive function and $q(x)$ is a nonnegative (but nonzero) smooth function. It follows that L is self-adjoint and positive definite.

Let $\langle \cdot, \cdot \rangle$ denote the standard inner product of functions defined on $[0, 2\pi]$,

$$\langle f(x), g(x) \rangle = \int_0^{2\pi} \overline{f(x)}g(x) dx. \quad (2.5)$$

Krylov subspace spectral methods, introduced in [18], use Gaussian quadrature on the spectral domain to compute the Fourier coefficients of the solution. These methods are time-stepping algorithms that compute the solution at time t_1, t_2, \dots , where $t_n = n\Delta t$ for some choice of Δt . Given the computed solution $\tilde{u}(x, t_n)$ at time t_n , the solution at time t_{n+1} is computed by approximating the Fourier coefficients that would be obtained by applying the exact solution operator to $\tilde{u}(x, t_n)$,

$$\hat{u}(\omega, t_{n+1}) = \left\langle \frac{1}{\sqrt{2\pi}} e^{i\omega x}, S(\Delta t)\tilde{u}(x, t_n) \right\rangle. \quad (2.6)$$

Krylov subspace spectral methods approximate these coefficients with higher-order temporal accuracy than traditional spectral methods and time-stepping schemes.

2.1 Elements of functions of matrices

In [7], Golub and Meurant describe a method for computing quantities of the form

$$\mathbf{u}^T f(A)\mathbf{v}, \quad (2.7)$$

where \mathbf{u} and \mathbf{v} are N -vectors, A is an $N \times N$ symmetric positive definite matrix, and f is a smooth function. Our goal is to apply this method with $A=L_N$ where L_N is a

spectral discretization of L , $f(\lambda)=\exp(-\lambda t)$ for some t , and the vectors \mathbf{u} and \mathbf{v} are derived from $\hat{\mathbf{e}}_\omega$ and \mathbf{u}^n , where $\hat{\mathbf{e}}_\omega$ is a discretization of

$$\frac{1}{\sqrt{2\pi}}e^{i\omega x},$$

and \mathbf{u}^n is the approximate solution at time t_n , evaluated on an N -point uniform grid.

The basic idea is as follows: since the matrix A is symmetric positive definite, it has real eigenvalues

$$b = \lambda_1 \geq \lambda_2 \geq \dots \geq \lambda_N = a > 0, \quad (2.8)$$

and corresponding orthogonal eigenvectors \mathbf{q}_j , $j = 1, \dots, N$. Therefore, the quantity (2.7) can be rewritten as

$$\mathbf{u}^T f(A) \mathbf{v} = \sum_{j=1}^N f(\lambda_j) \mathbf{u}^T \mathbf{q}_j \mathbf{q}_j^T \mathbf{v}. \quad (2.9)$$

We let $a=\lambda_N$ be the smallest eigenvalue, $b=\lambda_1$ be the largest eigenvalue, and define the measure $\alpha(\lambda)$ by

$$\alpha(\lambda) = \begin{cases} 0, & \text{if } \lambda < a, \\ \sum_{j=i}^N \alpha_j \beta_j, & \text{if } \lambda_i \leq \lambda < \lambda_{i-1}, \\ \sum_{j=1}^N \alpha_j \beta_j, & \text{if } b \leq \lambda, \end{cases} \quad (2.10)$$

where $\alpha_j=\mathbf{u}^T \mathbf{q}_j$ and $\beta_j=\mathbf{q}_j^T \mathbf{v}$. If this measure is positive and increasing, then the quantity (2.7) can be viewed as a Riemann-Stieltjes integral

$$\mathbf{u}^T f(A) \mathbf{v} = I[f] = \int_a^b f(\lambda) d\alpha(\lambda). \quad (2.11)$$

As discussed in [7], the integral $I[f]$ can be approximated using Gaussian quadrature rules, which yield an approximation of the form

$$I[f] = \sum_{j=1}^K w_j f(t_j) + R[f], \quad (2.12)$$

where the nodes t_j , $j = 1, \dots, K$, as well as the weights w_j , $j = 1, \dots, K$, can be obtained using the symmetric Lanczos algorithm if $\mathbf{u}=\mathbf{v}$, and the unsymmetric Lanczos algorithm if $\mathbf{u} \neq \mathbf{v}$ (see [10]).

2.2 Block Gaussian quadrature

In the case $\mathbf{u} \neq \mathbf{v}$, there is a possibility that the weights may not be positive, which destabilizes the quadrature rule (see [1] for details). One option to get around this problem is rewriting (2.7) using decompositions such as

$$\mathbf{u}^T f(A) \mathbf{v} = \frac{1}{\delta} [\mathbf{u}^T f(A) (\mathbf{u} + \delta \mathbf{v}) - \mathbf{u}^T f(A) \mathbf{u}], \quad (2.13)$$

where δ is a small constant. Guidelines for choosing an appropriate value for δ can be found in [18, Section 2.2].

If we compute (2.7) using (2.13) or the *polar decomposition*

$$\frac{1}{4} [(\mathbf{u} + \mathbf{v})^T f(A) (\mathbf{u} + \mathbf{v}) - (\mathbf{v} - \mathbf{u})^T f(A) (\mathbf{v} - \mathbf{u})], \quad (2.14)$$

then we could use the symmetric Lanczos algorithm, but we would still have to carry out the process for approximating an expression of the form (2.7) with two starting vectors. Instead, we consider

$$[\mathbf{u} \ \mathbf{v}]^T f(A) [\mathbf{u} \ \mathbf{v}], \quad (2.15)$$

which results in the 2×2 matrix

$$\int_a^b f(\lambda) d\mu(\lambda) = \begin{bmatrix} \mathbf{u}^T f(A) \mathbf{u} & \mathbf{u}^T f(A) \mathbf{v} \\ \mathbf{v}^T f(A) \mathbf{u} & \mathbf{v}^T f(A) \mathbf{v} \end{bmatrix}, \quad (2.16)$$

where $\mu(\lambda)$ is a 2×2 matrix function of λ , each entry of which is a measure of the form $\alpha(\lambda)$ from (2.10).

In [7], Golub and Meurant showed how a block method can be used to generate quadrature formulas. We will describe this process here in more detail. The integral

$$\int_a^b f(\lambda) d\mu(\lambda),$$

is now a 2×2 symmetric matrix and the most general K -node quadrature formula is of the form

$$\int_a^b f(\lambda) d\mu(\lambda) = \sum_{j=1}^K W_j f(T_j) W_j + error, \quad (2.17)$$

with T_j and W_j being symmetric 2×2 matrices. By diagonalizing each T_j , we obtain the simpler formula

$$\int_a^b f(\lambda) d\mu(\lambda) = \sum_{j=1}^{2K} f(\lambda_j) \mathbf{v}_j \mathbf{v}_j^T + error, \quad (2.18)$$

where for each j , λ_j is a scalar and \mathbf{v}_j is a 2-vector.

Each node λ_j is an eigenvalue of the matrix

$$\mathcal{T}_K = \begin{bmatrix} M_1 & B_1^T & & & & \\ B_1 & M_2 & B_2^T & & & \\ & \ddots & \ddots & \ddots & & \\ & & B_{K-2} & M_{K-1} & B_{K-1}^T & \\ & & & B_{K-1} & M_K & \end{bmatrix}, \quad (2.19)$$

which is a block-triangular matrix of order $2K$. The vector \mathbf{v}_j consists of the first two elements of the corresponding normalized eigenvector.

To compute the matrices M_j and B_j , we use the block Lanczos algorithm, which was proposed by Golub and Underwood in [9]. Let X_0 be an $N \times 2$ given matrix, such that $X_1^T X_1 = I_2$. Let $X_0 = 0$ be an $N \times 2$ matrix. Then, for $j = 1, \dots, K$, we compute

$$M_j = X_j^T A X_j, \quad R_j = A X_j - X_j M_j - X_{j-1} B_{j-1}^T, \quad X_{j+1} B_j = R_j. \quad (2.20)$$

The last step of the algorithm is the QR decomposition of R_j such that X_{j+1} is $n \times 2$ with

$$X_{j+1}^T X_{j+1} = I_2.$$

The matrix B_j is 2×2 and upper triangular. The other coefficient matrix M_j is 2×2 and symmetric.

2.3 Block KSS methods

We are now ready to describe block KSS methods. For each wave number $\omega = -N/2 + 1, \dots, N/2$, we define

$$R_0(\omega) = \begin{bmatrix} \hat{\mathbf{e}}_\omega & \mathbf{u}^n \end{bmatrix},$$

and compute the QR factorization $R_0(\omega) = X_1(\omega) B_0(\omega)$. We then carry out the block Lanczos iteration described in (2.20), applied to the discretized operator L_N , to obtain a block tridiagonal matrix $\mathcal{T}_K(\omega)$ of the form (2.19), where each entry is a function of ω .

Then, we can express each Fourier coefficient of the approximate solution at the next time step as

$$[\hat{\mathbf{u}}^{n+1}]_\omega = \left[B_0^H E_{12}^H \exp[-\mathcal{T}_K(\omega) \Delta t] E_{12} B_0 \right]_{12}, \quad (2.21)$$

where $E_{12} = \begin{bmatrix} \mathbf{e}_1 & \mathbf{e}_2 \end{bmatrix}$. The computation of (2.21) consists of computing the eigenvalues and eigenvectors of $\mathcal{T}_K(\omega)$ in order to obtain the nodes and weights for Gaussian quadrature, as described earlier.

This algorithm has local temporal accuracy $\mathcal{O}(\Delta t^{2K})$ [15]. Furthermore, block KSS methods are significantly more accurate than the original KSS methods described in [14, 18], that employ either (2.13) and (2.14), even though they have the same temporal order of accuracy, because the solution plays a greater role in the determination of the quadrature nodes. They are also more effective for problems with oscillatory or discontinuous coefficients.

3 Application to the wave equation

In this section, we review the application of Krylov subspace spectral methods to the problem

$$u_{tt} + Lu = 0, \quad \text{on } (0, 2\pi) \times (0, \infty), \quad (3.1)$$

$$u(x, 0) = f(x), \quad u_t(x, 0) = g(x), \quad 0 < x < 2\pi, \quad (3.2)$$

with periodic boundary conditions

$$u(0, t) = u(2\pi, t), \quad t > 0. \quad (3.3)$$

A spectral representation of the operator L allows us to obtain a representation of the solution operator (the *propagator*) in terms of the sine and cosine families generated by L by a simple functional calculus. Introduce

$$R_1(t) = L^{-1/2} \sin(t\sqrt{L}) = \sum_{n=1}^{\infty} \frac{\sin(t\sqrt{\lambda_n})}{\sqrt{\lambda_n}} \langle \varphi_n^*, \cdot \rangle \varphi_n, \quad (3.4)$$

$$R_0(t) = \cos(t\sqrt{L}) = \sum_{n=1}^{\infty} \cos(t\sqrt{\lambda_n}) \langle \varphi_n^*, \cdot \rangle \varphi_n, \quad (3.5)$$

where $\lambda_1, \lambda_2, \dots$ are the (positive) eigenvalues of L , and $\varphi_1, \varphi_2, \dots$ are the corresponding eigenfunctions. Then the propagator of (3.1) can be written as

$$P(t) = \begin{bmatrix} R_0(t) & R_1(t) \\ -LR_1(t) & R_0(t) \end{bmatrix}. \quad (3.6)$$

The entries of this matrix, as functions of L , indicate which functions are the integrands in the Riemann-Stieltjes integrals used to compute the Fourier coefficients of the solution.

Block KSS methods can be applied to the wave equation in the same way as for parabolic problems, as described in Section 2.3, except that the block Lanczos algorithm is used twice for each Fourier coefficient, to compute the solution and its time derivative.

We now review the convergence analysis of block KSS methods carried out in [16].

Theorem 1. *Let L be a self-adjoint 2nd-order positive definite differential operator on $C_p([0, 2\pi])$ with coefficients in $BL_M([0, 2\pi])$ for a fixed integer M , and let $f, g \in C_p^n([0, 2\pi])$ for $n \geq 4K + 1$ for a positive integer K . Let $N \geq M$, and that for each $\omega = -N/2 + 1, \dots, N/2$, the recursion coefficients in (2.19) are computed on a $2^K N$ -point uniform grid. Then a block KSS method that uses a K -node block Gaussian rule to compute each Fourier coefficient $[\hat{\mathbf{u}}^1]_\omega$, for $\omega = -N/2 + 1, \dots, N/2$, of the solution to (3.1), (3.2), (3.3), and each Fourier coefficient $[\hat{\mathbf{u}}_t^1]_\omega$ of its time derivative, satisfies*

$$\left| [\hat{\mathbf{u}}^1]_\omega - \hat{u}(\omega, \Delta t) \right| = \mathcal{O}(\Delta t^{4K}), \quad (3.7)$$

$$\left| [\hat{\mathbf{u}}_t^1]_\omega - \hat{u}_t(\omega, \Delta t) \right| = \mathcal{O}(\Delta t^{4K-1}), \quad (3.8)$$

where $\hat{u}(\omega, \Delta t)$ is the corresponding Fourier coefficient of the exact solution at time Δt .

Proof. See [16, Theorem 5]. □

In [16, Theorem 6], it is shown that when the leading coefficient $p(x)$ is constant and the coefficient $q(x)$ is bandlimited, the 1-node KSS method, which has third-order local accuracy in time, is also unconditionally stable. This result, and Theorem 1, imply convergence for the 1-node method, with second-order global temporal accuracy. In general, it follows from Theorem 1 that the local temporal error is $\mathcal{O}(\Delta t^{4K-2})$ when K block Gaussian nodes are used for each Fourier coefficient, and while it has not yet been proven, $\mathcal{O}(\Delta t^{4K-2})$ global temporal accuracy has been observed in numerical results (see [16]).

4 Application to Maxwell’s equations

In this section, we consider the various generalizations that must be made to block KSS methods for the wave equation in order to apply them to Maxwell’s equations, and then discuss the performance of the resulting algorithm.

4.1 Generalization to Systems of Equations

First, we consider the following initial-boundary value problem in one space dimension,

$$\frac{\partial^2 \mathbf{u}}{\partial t^2} + L\mathbf{u} = 0, \quad t > 0, \tag{4.1}$$

$$\mathbf{u}(x, 0) = \mathbf{f}(x), \quad \frac{\partial \mathbf{u}}{\partial t}(x, 0) = \mathbf{g}(x), \quad 0 < x < 2\pi, \tag{4.2}$$

with periodic boundary conditions

$$\mathbf{u}(0, t) = \mathbf{u}(2\pi, t), \quad t > 0, \tag{4.3}$$

where

$$\mathbf{u} : [0, 2\pi] \times [0, \infty) \rightarrow \mathbb{R}^n, \quad \text{for } n > 1,$$

and $L(x, D)$ is an $n \times n$ matrix where the (i, j) entry is an a differential operator $L_{ij}(x, D)$ of the form

$$L_{ij}(x, D)u(x) = \sum_{\mu=0}^{m_{ij}} a_{\mu}^{ij}(x)D^{\mu}u, \quad D = \frac{d}{dx}, \tag{4.4}$$

with spatially varying coefficients $a_{\mu}^{ij}, \mu = 0, 1, \dots, m_{ij}$.

Generalization of KSS methods to a system of the form (4.1) can proceed as follows. For $i, j = 1, \dots, n$, let $\bar{L}_{ij}(D)$ be the constant-coefficient operator obtained by averaging the coefficients of $L_{ij}(x, D)$ over $[0, 2\pi]$. Then, for each wave number ω , we define

$L(\omega)$ be the matrix with entries $\bar{L}_{ij}(\omega)$, i.e., the symbols of $\bar{L}_{ij}(D)$ evaluated at ω . Next, we compute the spectral decomposition of $L(\omega)$ for each ω . For $j = 1, \dots, n$, let $\mathbf{q}_j(\omega)$ be the Schur vectors of $L(\omega)$. Then, we define our test and trial functions by

$$\vec{\phi}_{j,\omega}(x) = \mathbf{q}_j(\omega) \otimes e^{i\omega x}.$$

The recursion coefficients, nodes and weights can be computed in the same manner as in the scalar, self-adjoint case, with obvious modifications to account for the fact that the matrix $T_\omega(\delta_\omega)$, for each ω , is no longer Hermitian. Once the coefficients of the solution in our basis of trial functions is computed, the Fourier coefficients of each component function can be computed by solving nN linear systems of size $n \times n$.

4.2 Implementation

In [19], it was demonstrated that recursion coefficients for all wave numbers $\omega = -N/2 + 1, \dots, N/2$ can be computed simultaneously, by regarding them as functions of ω and using symbolic calculus to apply differential operators analytically, as much as possible. As a result, KSS methods require $\mathcal{O}(N \log N)$ floating-point operations per time step, which is comparable to other time-stepping methods. The same approach can be applied to block KSS methods. For both types of methods, it can be shown that for a K -node Gaussian rule or block Gaussian rule, K applications of the operator L_N to the previous solution \mathbf{u}^n , and its time derivative, are needed.

To facilitate this analytic precomputation of recursion coefficients, we can represent Lanczos vectors as linear combinations of functions such as the solution from the previous time steps, premultiplied by zero or more powers of L_N , and products of functions with $\hat{e}_\omega(x)$, and the dependence of the Lanczos vectors, or inner products of them, on ω is reflected in the coefficients of the functions in these linear combinations. Details are given in [17].

4.3 Higher space dimension

In [19], it is demonstrated how to compute the recursion coefficients α_j and β_j for operators of the form

$$Lu = -p\Delta u + q(x, y)u,$$

and the expressions are straightforward generalizations of the expressions for the one-dimensional case. It is therefore reasonable to suggest that for operators of this form, the consistency and stability results given here for the one-dimensional case generalize to higher dimensions. This will be investigated in the near future. The implementation details above generalize in a straightforward manner, but because of the additional memory required, it is particularly important to eliminate any redundant computation, which can be accomplished by representing recursion coefficients as expression trees.

4.4 Discontinuous coefficients and data

As shown in [16, 19], rough or discontinuous coefficients reduce the accuracy of KSS methods, because they introduce significant spatial discretization error into the computation of recursion coefficients.

Ongoing work, described in [17], involves the use of the polar decomposition (2.14), to alleviate difficulties caused by such coefficients and initial data. This approach uses symmetric perturbations of initial Lanczos vectors in the direction of the solution in order to cancel out high-frequency oscillations. Future work will explore possible combinations of this approach with block KSS methods in order to generalize the superior accuracy of the block approach to these more difficult problems.

Alternatively, adaptive spatial resolution has been shown to be effective for handling multilayer profiles in TE and TM polarizations (see [25]), which KSS methods can readily incorporate as well. Ongoing work also explores the use of reprojection techniques (see, e.g., [6]).

4.5 Other boundary conditions

While we have used periodic boundary conditions in this paper, it is typical in practical applications to use boundary conditions that are more effective at simulating an infinite domain. One such type of boundary condition is a perfectly matched layer (PML), first used by Berenger in [3] for Maxwell's equations. A PML absorbs waves by modifying spatial differentiation operators in the PDE. For example, for absorbing waves that propagate in the x direction, $\partial/\partial x$ is replaced by

$$\frac{1}{1 + \frac{i\sigma(x)}{\omega}} \frac{\partial}{\partial x'}$$

where, as before, ω represents the wave number, and σ is a positive function that causes propagating waves to be attenuated.

In KSS methods, this transformation can be incorporated into the symbol of the operator L when computing the recursion coefficients. The dependence of the transformation on both x and ω makes the efficient application of the transformed operator more difficult, especially in higher space dimensions, but recent work on rapid application of Fourier integral operators (see [4]) can mitigate this concern. Future work will explore the use of PML, taking into account very recent analysis in [21] of the difficulties of PML with inhomogeneous media, and the remediation of these difficulties through adiabatic absorbers.

4.6 Non-self-adjoint differential operators

For Maxwell's equations, the matrix A_N that discretizes the operator

$$A\hat{\mathbf{E}} = \frac{1}{\mu\epsilon} \left(\Delta\hat{\mathbf{E}} + \mu^{-1} \text{curl} \hat{\mathbf{E}} \times \nabla\mu \right),$$

is not symmetric, and for each coefficient of the solution, the resulting quadrature nodes λ_j , $j = 1, \dots, 2K$, from (2.18) are now complex and must be obtained by a straightforward modification of block Lanczos iteration for unsymmetric matrices, in which the process (2.20) is replaced by

$$M_j = Y_j^H A X_j, \quad R_j = A X_j - X_j M_j - X_{j-1} C_{j-1}^H, \quad (4.5)$$

$$P_j = A^H Y_j - Y_j M_j^H - Y_{j-1} B_{j-1}^H, \quad P_j^H R_j = C_j^H B_j, \quad (4.6)$$

$$X_{j+1} B_j = R_j, \quad Y_{j+1} C_j = P_j, \quad (4.7)$$

where $P_0=R_0$ and both B_j and C_j are upper triangular. The above equation allows flexibility in the computation of B_j and C_j . We arbitrarily impose the additional constraint that their main diagonals be complex conjugates of one another.

4.7 Accuracy and stability

Let A be a symmetric matrix with eigenvalues (2.8). The error $R[f]$ in the approximation of $\mathbf{u}^T f(A) \mathbf{v}$ by a quadrature rule of the form (2.18) is given by

$$R[f] = \frac{1}{(2K)!} \int_a^b \frac{d^{2K} f(\xi(\lambda))}{d\lambda^{2K}} \prod_{j=1}^{2K} (\lambda - \lambda_j) d\alpha(\lambda), \quad (4.8)$$

where $\alpha(\lambda)$ is as defined in (2.10) and $a < \xi(\lambda) < b$ for $a < \lambda < b$. It is the differentiation of the integrand f , which depends on Δt in KSS methods, that yields their high-order accuracy in time.

Because A is not symmetric when obtained by discretizing Maxwell's equations, the integral (4.8) is defined on a contour in the complex plane that passes through the eigenvalues of A , as discussed in [23]. Future work will include detailed analysis of the quadrature error, but what we can readily observe from this error is that the dependence of this error on Δt is the same as in the symmetric case, which bodes well for application to Maxwell's equations.

More specifically, suppose that we use an N -point grid in each spatial dimension. Generalizing the discussion in Section 4.1, our basis of trial functions is defined by

$$\vec{u}_{j,\vec{\omega}}(\mathbf{x}) = \mathbf{q}_j(\vec{\omega}) \otimes e^{i\vec{\omega} \cdot \mathbf{x}} \equiv \begin{bmatrix} Q_{1j}^{\vec{\omega}} e^{i\vec{\omega} \cdot \mathbf{x}} \\ Q_{2j}^{\vec{\omega}} e^{i\vec{\omega} \cdot \mathbf{x}} \\ Q_{3j}^{\vec{\omega}} e^{i\vec{\omega} \cdot \mathbf{x}} \end{bmatrix}, \quad (4.9)$$

where $\mathbf{x} \in [0, 2\pi]^3$ and $\vec{\omega} = (\omega_1, \omega_2, \omega_3)$, with $\omega_i = -N/2 + 1, \dots, N/2$ for $i = 1, 2, 3$. We denote the discretization of $\vec{u}_{j,\vec{\omega}}$ on the grid by the $3N^3$ -vector $\mathbf{u}_{j,\vec{\omega}}$. Then, applying (4.8) and (3.6), the error in each Fourier coefficient of each component of the computed

solution $\mathbf{E}^1 = (\mathbf{E}_1^1, \mathbf{E}_2^1, \mathbf{E}_3^1)$, which approximates the electric field $\mathbf{E}(\mathbf{x}, \Delta t)$, is given by

$$\begin{aligned}
 [\mathcal{E}_i^1]_{\vec{\omega}} &= \hat{E}_i(\vec{\omega}, \Delta t) - [\mathbf{E}_i^1]_{\vec{\omega}} \\
 &= \sum_{j=1}^3 Q_{ij}^{\vec{\omega}} \mathbf{u}_{j,\vec{\omega}}^H [R_{K,j,\vec{\omega}}(A_N) \mathbf{E}^0 + \tilde{R}_{K,j,\vec{\omega}}(A_N) \mathbf{E}_t^0] \\
 &= \sum_{j=1}^3 Q_{ij}^{\vec{\omega}} \sum_{k,\ell=1}^3 Q_{kj}^{\vec{\omega}} \hat{\mathbf{e}}_{\vec{\omega}}^H [R_{K,j,\vec{\omega}}^{k\ell}(A_N) \mathbf{E}_\ell^0 + \tilde{R}_{K,j,\vec{\omega}}^{k\ell}(A_N) [\mathbf{E}_t^0]_\ell], \tag{4.10}
 \end{aligned}$$

where the matrix function $R_{K,j,\vec{\omega}}(A_N)$ is defined by

$$R_{K,j,\vec{\omega}}(\lambda) = \frac{1}{(2K)!} \frac{d^{2K}}{d\lambda^{2K}} [\cos(\sqrt{\lambda}\Delta t)] \Big|_{\lambda=\xi(\lambda)} \prod_{k=1}^{2K} (\lambda - \lambda_k^{j,\vec{\omega}}), \tag{4.11}$$

and $R_{K,j,\vec{\omega}}^{k\ell}(A_N)$ is the (k, ℓ) block of $R_{K,j,\vec{\omega}}(A_N)$, where each block is $N^3 \times N^3$. The superscript $j, \vec{\omega}$ for λ_k indicates the dependence of the scalar quadrature nodes λ_k from (2.18) on j and $\vec{\omega}$. The matrices $\tilde{R}_{K,j,\vec{\omega}}(A_N)$ and $\tilde{R}_{K,j,\vec{\omega}}^{k\ell}(A_N)$ are defined analogously, with $\cos(\sqrt{\lambda}\Delta t)$ replaced by $\lambda^{-1/2} \sin(\sqrt{\lambda}\Delta t)$, in view of (3.6). We also note that because the trial functions are constructed using Schur vectors, the constants $Q_{ij}^{\vec{\omega}}$ are entries of a 3×3 unitary matrix, for each j and $\vec{\omega}$.

As in the case of the scalar wave equation, the differentiation with respect to λ of the integrands $\cos(\sqrt{\lambda}\Delta t)$ and $\lambda^{-1/2} \sin(\sqrt{\lambda}\Delta t)$ in (4.11) and its analogue for $\tilde{R}_{K,j,\vec{\omega}}(A_N)$ introduces factors of Δt^{4K} and Δt^{4K+1} , respectively, for these two integrands. Similarly, factors of Δt^{4K-1} and Δt^{4K} are introduced by differentiation of the integrands used to compute Fourier coefficients of the time derivative of the solution. We therefore expect $\mathcal{O}(\Delta t^{4K-2})$ temporal accuracy, as has been obtained for the scalar wave equation.

This result is more difficult to prove than for the wave equation, because A_N is not symmetric, and therefore we do not do this here. However, it is helpful to note that the high degree of accuracy of block Gaussian quadrature for approximating (2.15) can be shown to extend to unsymmetric matrices, by showing directly that the leading 2×2 block of

$$A_N [X_1 \ \cdots \ X_K] - [X_1 \ \cdots \ X_K] f(\mathcal{T}_K),$$

vanishes, when f is a polynomial of degree less than $2K$, provided that the unsymmetric Lanczos iteration does not suffer from serious breakdown (see [12] for discussion of standard Gaussian quadrature applied to (2.7) in the unsymmetric case).

Although KSS methods are explicit, they are not constrained by a CFL condition. This is due to the fact that the CFL condition is derived from the requirement that the domain of dependence of the numerical scheme contains that of the PDE, but the computation of the recursion coefficients in $\mathcal{T}_K(\omega)$, for each ω , uses values of the solution on the entire spatial domain. Further stability analysis is deferred to future work.

5 Numerical results

In this section, we apply block KSS methods to Maxwell's equations in two and three spatial dimensions.

5.1 Two-dimensional problems

We first consider a two-dimensional version of (1.3), for the electric field $\hat{\mathbf{E}}=(E_x, E_y)$, where μ is independent of z :

$$\mu\varepsilon\frac{\partial^2 E_x}{\partial t^2} = \Delta E_x + \frac{1}{\mu}\frac{\partial\mu}{\partial y}\left(\frac{\partial E_x}{\partial y} - \frac{\partial E_y}{\partial x}\right), \quad (5.1)$$

$$\mu\varepsilon\frac{\partial^2 E_y}{\partial t^2} = \Delta E_y + \frac{1}{\mu}\frac{\partial\mu}{\partial x}\left(\frac{\partial E_y}{\partial x} - \frac{\partial E_x}{\partial y}\right), \quad (5.2)$$

$$\hat{\mathbf{E}}(x, y, 0) = \mathbf{F}(x, y), \quad \frac{\partial\hat{\mathbf{E}}}{\partial t}(x, y, 0) = \mathbf{G}(x, y), \quad (5.3)$$

with periodic boundary conditions. The coefficients μ and ε are constructed from randomly generated, damped Fourier coefficients as described in [18]. Specifically,

$$\begin{aligned} \mu(x, y) = & 0.4154 + 0.0125 \cos y + 0.0024 \sin y + 0.0054 \cos x + 0.0028 \sin x \\ & + 0.0067 \cos(x - y), \end{aligned} \quad (5.4)$$

$$\varepsilon(x, y) = 0.4138 + 0.0044 \cos y + 0.0049 \sin y + 0.004 \cos x + 0.0059 \sin x. \quad (5.5)$$

Both functions are shown in Fig. 1.

Table 1 and Fig. 2 demonstrate the convergence behavior using error estimates for solutions computed at various grid spacings and time steps, with $K=2$ block quadrature nodes per coefficient in the basis described in Section 4.1. Since the exact solution is unknown, the error estimate for each solution is obtained by taking the ℓ_2 -norm of

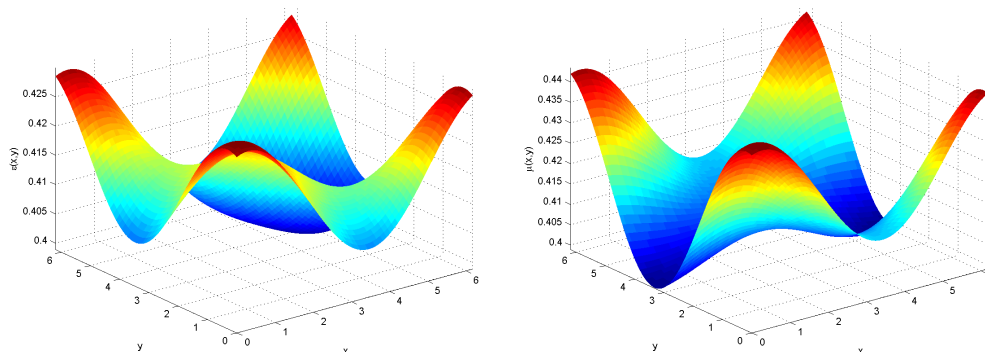


Figure 1: The coefficients in (5.1), (5.2), defined in (5.4), (5.5): (left) $\varepsilon(x, y)$, (right) $\mu(x, y)$

Table 1: Estimates of relative error in solutions of (5.1), (5.2), (5.3) computed using a 2-node block KSS method on an N -point grid, with time step Δt , for various values of N and Δt .

Δt	$N = 16$	$N = 32$	$N = 64$
1	5.799e-4	5.799e-4	5.799e-4
1/2	3.038e-5	3.038e-5	3.038e-5
1/4	4.230e-7	4.223e-7	4.223e-7
1/8	2.063e-8	6.020e-9	6.020e-9
1/16	2.171e-8	8.502e-11	8.502e-11
1/32	2.592e-8	1.561e-12	1.350e-12

the relative difference between the x -components of the solution, and a solution computed using a smaller time step $\Delta t=1/64$ and the maximum number of grid points.

At all three spatial resolutions, the scheme exhibits approximately 6th-order accuracy in time as Δt decreases below 1/2, except that for $N=16$, the spatial error arising from truncation of Fourier series is significant enough that the overall error fails to decrease below the level achieved at $\Delta t=1/8$. For $N=32$ and $N=64$, the solution is sufficiently resolved in space, and the order of overconvergence as $\Delta t \rightarrow 0$ is approximately 6.1.

We also note that increasing the resolution does not pose any difficulty from a stability point of view. Unlike explicit finite-difference schemes that are constrained by a CFL condition, KSS methods do not require a reduction in the time step to offset a reduction in the spatial step in order to maintain boundedness of the solution.

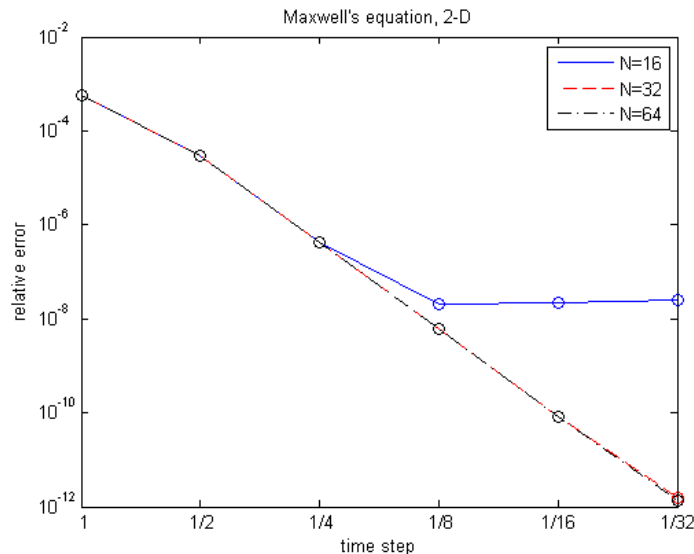


Figure 2: Estimates of relative error in solutions of (5.1), (5.2), (5.3) computed using a 2-node block KSS method on an N -point grid, with time step Δt , for various values of N and Δt .

5.2 Three-dimensional problems

We now apply a 2-node block KSS method to Eq. (1.3), with initial conditions

$$\hat{\mathbf{E}}(x, y, z, 0) = \mathbf{F}(x, y, z), \quad \frac{\partial \hat{\mathbf{E}}}{\partial t}(x, y, z, 0) = \mathbf{G}(x, y, z), \quad (5.6)$$

with periodic boundary conditions. The coefficients $\mu(x, y, z)$ and $\varepsilon(x, y, z)$ are defined as in Section 5.1, and are given by

$$\begin{aligned} \mu(x, y, z) = & 0.4077 + 0.0039 \cos z + 0.0043 \cos y - 0.0012 \sin y \\ & + 0.0018 \cos(y + z) + 0.0027 \cos(y - z) + 0.003 \cos x \\ & + 0.0013 \cos(x - z) + 0.0012 \sin(x - z) \\ & + 0.0017 \cos(x + y) + 0.0014 \cos(x - y), \end{aligned} \quad (5.7)$$

$$\begin{aligned} \varepsilon(x, y, z) = & 0.4065 + 0.0025 \cos z + 0.0042 \cos y + 0.001 \cos(y + z) \\ & + 0.0017 \cos x + 0.0011 \cos(x - z) \\ & + 0.0018 \cos(x + y) + 0.002 \cos(x - y). \end{aligned} \quad (5.8)$$

The components of \mathbf{F} and \mathbf{G} are generated in a similar fashion, except that the x - and z -components are zero.

Table 2 and Fig. 3 demonstrate the convergence behavior using error estimates for solutions computed using $K=2$ block quadrature nodes per coefficient in the basis described in Section 4.1. As before, the error estimate for each solution is obtained by taking the ℓ_2 -norm of the relative difference between the y -component of the solution, and that of a solution computed using a smaller time step $\Delta t=1/64$ and the maximum number of grid points. We observe similar qualitative behavior, for decreasing Δt and increasing N , as in the two-dimensional case.

In a few cases, for larger values of Δt , there are slight increases in the error as N , the number of grid points per dimension is doubled. This is due to the inclusion of higher-frequency components that, for larger Δt , are not computed with sufficient accuracy. Although the initial data and coefficients are bandlimited, the solution is not, due to the heterogeneity of the coefficients, thus allowing these higher-frequency errors to be

Table 2: Estimates of relative error in solutions of (1.3), (5.6) computed using a 2-node block KSS method on an N -point grid, with time step Δt , for various values of N and Δt .

Δt	$N = 16$	$N = 32$
1	1.608e-2	1.609e-2
1/2	2.249e-4	2.250e-4
1/4	1.563e-6	1.563e-6
1/8	3.382e-8	1.794e-8
1/16	2.108e-8	2.026e-10
1/32	2.101e-8	2.721e-12

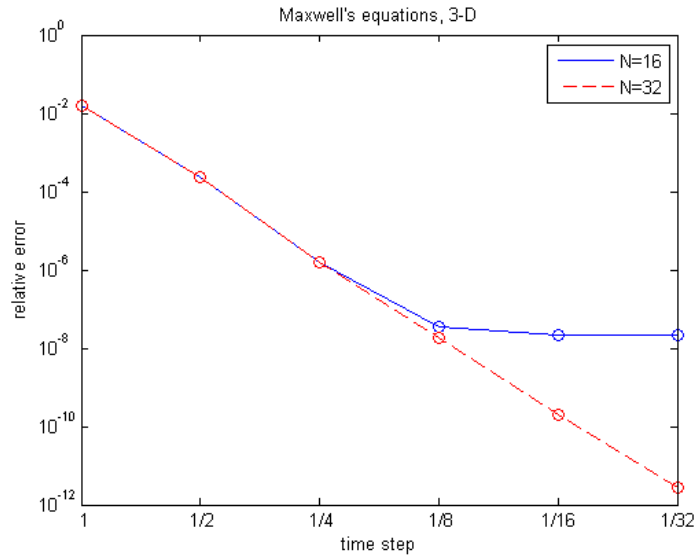


Figure 3: Estimates of relative error in solutions of (1.3), (5.6) computed using a 2-node block KSS method on an N -point grid, with time step Δt , for various values of N and Δt .

introduced. As Δt decreases, these higher-frequency components are resolved with sufficient accuracy to yield the expected decrease in error as N increases.

We tried solving this same problem with MATLAB's most accurate ODE solvers, `ode45` and `ode15s`, the algorithms for which are described in [24]. This is accomplished by rewriting (1.3) as a first-order system for the components of $\hat{\mathbf{E}}$ and its time derivative. Unfortunately, `ode15s` used too much memory and failed to produce a solution. Accurate results could be obtained for `ode45` for the coarser grid, and these were comparable to the results obtained by KSS methods, although the order of accuracy was slightly less. However, as N increased, `ode45` was unable to obtain reasonable accuracy for the same time steps, due to instability. Future analysis will include comparisons of KSS methods and competing methods, implemented in compiled languages, as comparison of execution time in MATLAB can be misleading (see [19]).

6 Conclusions

We have demonstrated that KSS methods can be applied to Maxwell's equations with smoothly varying coefficients. The order of temporal accuracy is the same as for the wave equation, even though Fourier coefficients are now represented by bilinear forms involving non-self-adjoint matrices, which are treated as Riemann-Stieltjes integrals over contours in the complex plane. Future work will extend the approach described in this paper to more realistic applications by using symbol modification to efficiently implement perfectly matched layers, and various techniques to effectively handle discontinuous coefficients.

Acknowledgments

The author thanks John J. Hench and Zdeněk Strakoš for the introduction to computational electrodynamics, as well as helpful and stimulating discussions.

References

- [1] K. ATKINSON, *An Introduction to Numerical Analysis*, 2nd Ed., Wiley, 1989.
- [2] S. BASU AND N. K. BOSE, *Matrix Stieltjes series and network models*, SIAM J. Math. Anal., 14 (1983), pp. 209–222.
- [3] J. BERENGER, *A perfectly matched layer for the absorption of electromagnetic waves*, J. Comp. Phys., 114 (1994), pp. 185–200.
- [4] E. CANDÈS, L. DEMANET AND L. YING, *Fast computation of Fourier integral operators*, SIAM J. Sci. Comput., 29 (2007), pp. 2464–2493.
- [5] H. DE RAEDT, K. MICHIENSEN, J. S. KOLE AND M. T. FIGGE, *Solving the Maxwell equations by the Chebyshev method: A one-step finite difference time-domain algorithm*, Ant. Prop., IEEE Trans., 51 (2003), pp. 3155–3160.
- [6] A. GELB AND J. TANNER, *Robust reprojection methods for the resolution of the Gibbs phenomenon*, Appl. Comput. Harmon. Anal., 20 (2006), pp. 3–25.
- [7] G. H. GOLUB AND G. MEURANT, *Matrices, moments and quadrature*, Proceedings of the 15th Dundee Conference, June-July 1993, D. F. Griffiths, G. A. Watson (eds.), Longman Scientific & Technical (1994).
- [8] G. H. GOLUB AND M. H. GUTKNECHT, *Modified moments for indefinite weight functions*, Numerische Mathematik, 57 (1989), pp. 607–624.
- [9] G. H. GOLUB AND R. UNDERWOOD, *The block Lanczos method for computing eigenvalues*, Mathematical Software III, J. Rice Ed., (1977), pp. 361–377.
- [10] G. H. GOLUB AND J. WELSCH, *Calculation of Gauss quadrature rules*, Math. Comp., 23 (1969), pp. 221–230.
- [11] P. GUIDOTTI, J. V. LAMBERS AND K. SØLNA, *Analysis of 1-D wave propagation in inhomogeneous media*, Numer. Fun. Anal. Optim., 27 (2006), pp. 25–55.
- [12] H. GUO AND R. A. RENAULT, *Estimation of $\mathbf{u}^T f(A) \mathbf{v}$ for large-scale unsymmetric matrices*, Numer. Linear Algebr., 11 (2004), pp. 75–89.
- [13] M. HOCHBRUCK AND C. LUBICH, *On Krylov Subspace Approximations to the Matrix Exponential Operator*, SIAM J. Numer. Ana., 34 (1996), pp. 1911–1925.
- [14] J. V. LAMBERS, *Derivation of high-order spectral methods for time-dependent PDE using modified moments*, Electron. Numer. Ana., 28 (2008), pp. 114–135.
- [15] J. V. LAMBERS, *Enhancement of Krylov subspace spectral methods by block Lanczos iteration*, Electron. Numer. Ana., 31 (2008), pp. 86–109.
- [16] J. V. LAMBERS, *An explicit, stable, high-order spectral method for the wave equation based on block Gaussian quadrature*, IAENG J. Appl. Math., 38 (2008), pp. 333–348.
- [17] J. V. LAMBERS, *Krylov subspace spectral methods for the time-dependent Schrödinger equation with non-smooth potentials*, Numer. Algorith., 51 (2009), pp. 239–280.
- [18] J. V. LAMBERS, *Krylov subspace spectral methods for variable-coefficient initial-boundary value problems*, Electron. Tran. Numer. Ana., 20 (2005), pp. 212–234.
- [19] J. V. LAMBERS, *Practical implementation of Krylov subspace spectral methods*, J. Sci. Comput., 32 (2007), pp. 449–476.

- [20] Q. H. LIU, *The pseudospectral time-domain (PSTD) method: A new algorithm for solutions of Maxwell's equations*, Ant. Prop. Soc. Int'l Symp. Dig., IEEE, 1 (1997), pp. 122–125.
- [21] A. F. OSKOOL, L. ZHANG, Y. AVNIEL AND S. G. JOHNSON, *The failure of perfectly matched layers, and towards their redemption by adiabatic absorbers*, Opt. Expr., 16 (2008), pp. 11376–11392.
- [22] T. RYLANDER AND A. BONDESON, *Stable FDTD-FEM hybrid method for Maxwell's equations*, Comp. Phys. Comm., 125 (2000), pp. 75–82.
- [23] P. E. SAYLOR AND D. C. SMOLARSKI, *Why Gaussian quadrature in the complex plane?*, Numer. Alg., 26 (2001), pp. 251–280.
- [24] L. F. SHAMPINE AND M. W. REICHELT, *The MATLAB ODE suite*, SIAM J. Sci. Comput., 18 (1997), pp. 1–22.
- [25] T. VALLIUS AND M. HONKANEN, *Reformulation of the Fourier nodal method with adaptive spatial resolution: application to multilevel profiles*, Opt. Expr., 10 (2002), pp. 24–34.
- [26] K. YEE, *Numerical solution of initial boundary value problems involving Maxwell's equations in isotropic media*, Ant. Prop., IEEE Trans., 14 (1966), pp. 302–307.